Gold Nanoparticles Alleviate Meloxicam Induced Toxicity in Adult Male Rat Spleen through Activation of Autophagy: Histological and Immunohistochemical Study

Original Article

Sherine Ahmed Mohammed[1], Hekmat Osman Abdel Aziz[1], Aziz Awaad[2] and Samira Mahmoud Mohamed[1]

[1]Department of Histology, [2]Department of Zoology, Faculty of Medicine, Sohag University, Sohag, Egypt

ABSTRACT

Background: Meloxicam is an analgesic with higher selective inhibition of cyclooxygenase 2 (COX-2). COX-2 inhibition induces oxidative stress. Gold nanoparticles (AuNPs) have several medical applications in diagnosing and treating diseases and have potent free radical scavenging properties.

Objective: This study was conducted to assess the possible therapeutic effect of AuNPs on meloxicam-induced splenic toxicity at different time points.

Materials and Methods: Forty-five rats were used in this experiment and were divided into eight groups: group I; the control group. Group II received AuNPs for 2 weeks. Groups III and IV received meloxicam for 2 weeks and 2 months respectively. Groups V and VI received AuNPs for 2 weeks after receiving meloxicam for 2 weeks and 2 months respectively. Groups VII and VIII received meloxicam for two weeks and 2 months respectively followed by cessation of treatment for 2 weeks. Both meloxicam and AuNPs were injected daily intraperitoneally in a dose of 15mg/kg and 50 ul respectively. Histological changes, AuNPs localization in the spleen by silver nitrate, PCNA immunoexpression to detect cellular proliferation, and LC3 and p62 for detecting autophagy activation were studied.

Results: Time-dependent degenerative histological changes and increased PCNA, LC3, and p62 expression were observed after meloxicam treatment. However, AuNPs ameliorated these changes.

Conclusions: AuNPs have a therapeutic role against the toxic effects of meloxicam in the spleen which may be due to their antioxidant activity, in addition to activation of autophagy.

Key Words: AuNPs, Autophagy, Gold nanoparticles, Meloxicam.

Revised: 08 December 2022, **Accepted:** 17 January 2023

Corresponding Author: *Sherine Ahmed Mohammed*, *Department of Histology, Faculty of Medicine, Sohag University, Sohag, Egypt,* **Tel.:** *+201120301020*, **E-mail:** *sherinahmed@med.sohag.edu.eg.*

ISSN: 1110-0559, Vol. , No.

INTRODUCTION

Meloxicam is a non-steroidal anti-inflammatory drug (NSAID) and is the drug of choice in the treatment of rheumatic diseases and other inflammatory joint diseases. It is recommended to use NSAIDs for the shortest duration. Meloxicam has selective inhibition of cyclooxygenase 2 (COX-2). The COX-2 enzyme is widely distributed in blood vessels and plays an important role in keeping physiological balance. Prolonged COX-2 inhibition induces oxidative stress[1].

Oxidative stress is a condition that disturbs the oxidant/antioxidant balance as a result of a significant rise in reactive oxygen species in cells and a decline in antioxidant levels which leads to lipid peroxidation and cellular degeneration[2]. The spleen is considered a strategic organ in the drainage of many drugs including meloxicam[3].

Gold nanoparticles (AuNPs) have several applications in the diagnosis and treatment of diseases such as targeted drug delivery[4]. AuNPs have potent free radical scavenging properties. This may be due to their ability to neutralize free radicals. When their concentration is increased, free radical scavenging ability is directly increased[5].

AuNPs were proven to have a role in autophagy modulation. Autophagy is essential for cell survival and counteracting cellular stress by getting rid of degenerated cell components. However, excessive stimulation of autophagy or blockage of its flux could cause disturbance of the cellular system[6].

AuNPs are uptaken by the reticuloendothelial system. So, the major organs of AuNPs accumulation were the liver and spleen because of the presence of numerous resident macrophages[7]. This study was conducted to assess the possible therapeutic effect

Personal non-commercial use only. JMH copyright © 2017. All rights eserved *DOI: 10.21608/jmh.2023.179541.1110*

of AuNPs (50 ul) on meloxicam-induced splenic toxicity in a dose of (15 mg/kg) at different time points.

MATERIALS AND METHODS

Animals:

Forty-five adult male albino rats (23- months) old were used in this study. The body weight of each animal was 200250- grams. The rats were kept at a suitable temperature and well-ventilated animal house in the Faculty of Medicine, Sohag University under natural photoperiod conditions and had free access to food and water during the experiment. All conditions were approved by the ethical committee of Sohag faculty of medicine IRB00013006, Sohag -IACUC - 5 - 11 - 2022 - 2.

Chemicals:

i. Gold nanoparticles (510- nm): were purchased from Sigma Aldrich Company, Germany.

ii. Meloxicam: was purchased from Delta-Pharma.

iii. Silver nitrate kits: were purchased from Sigma Aldrich Company, Germany.

iv. P62/SQSTM1 mouse monoclonal antibody (E-AB-27287, 1/ 100, for detection of autophagy); Elabscience company.

v. LC3 B mouse monoclonal antibody (E-AB-33747, 1/ 100, for detection of autophagy); Elabscience company.

vi. Mouse monoclonal proliferating cell nuclear antigen (PCNA) antibody (Ab-1, pc10,1 /400, for detection of cell regeneration NA03) Sigma-Aldrich.

Experimental design:

Forty-five rats were used in this experiment and were divided into eight groups:

Group I: Control group, 10 rats were treated with saline, 5 of them for two weeks (subgroup 1a) and the other five for two months (subgroup 1b).

Group II: 5 rats were injected with gold nanoparticles (50 ul) intraperitoneally daily for 2weeks (8).

Group III: 5 rats received meloxicam in a dose of (15 mg/kg) intraperitoneally daily for 2 weeks.

Group IV: 5 rats received meloxicam in a dose of (15 mg/kg) intraperitoneally daily for 2 months.

Group V: 5 rats received meloxicam in a dose of (15 mg/kg) intraperitoneally daily for 2 weeks then AuNPs (50 ul) intraperitoneally daily for the subsequent 2 weeks with stopping meloxicam[8].

Group VI: 5 rats received meloxicam in a dose of (15 mg/kg) intraperitoneally daily for 2 months then AuNPs (50 ul) intraperitoneally daily for the subsequent 2 weeks with stopping the injection of meloxicam[8].

Group VII: (meloxicam control): 5 rats were given meloxicam (15 mg/kg) intraperitoneally daily for 2 weeks then saline for the subsequent 2 weeks with stopping the injection of meloxicam.

Group VIII: (meloxicam control): 5 rats received meloxicam in a dose of (15 mg/kg) intraperitoneally daily for 2 months then saline for the subsequent 2 weeks with stopping meloxicam.

Histological studies:

At the end of the experiment, the animals were anesthetized by intraperitoneal injection of ketamine 85 mg/kg plus 8 mg/ kg xylazine[9]. The spleen was dissected and cut into small pieces. Samples from all groups were immediately fixed in 10 % formalin, processed and embedded in paraffin blocks and were sliced using a microtome (5 µm sections). Sections were mounted on glass slides and then stained with:

i. Hematoxylin and eosin stain (H& E): for general histological studies. the used staining method was applied according to Bancroft[10].

ii. Silver nitrate stain: was used for the localization enhancement of AuNPs in tissues[11].

Immunohistochemical studies:

The labeled streptavidin-biotin method was performed using anti-polyvalent HRD/DAP plus Labvision detection system. Tissue paraffin embedded 5 µm thick sections were performed on coated glass slides. The slides were deparaffinized in xylene and rehydrated. Endogenous peroxidase blockage was done using 0.3 % hydrogen peroxide for 10 minutes. Antigen retrieval was done by boiling slides at a high temperature (80°C) for 10 min in citrate buffer solution (pH 6.0) using a microwave oven. Incubation of the slides with the primary antibody (1:100 dilution for LC3 and P62, 1:400 dilution for PCNA) was done at 4°C for

18 – 20h. After that, biotinylated secondary antibodies and then the avidin-biotin complex was applied to the slides at room temperature and the staining was visualized with diaminobenzidine and chromogen. The sections were finally counterstained with hematoxylin. Then, dehydrated, cleared and mounted[12]. Negative control slides were done with the omission of the 1ry antibodies. Positivity appeared as brown coloration. Positive control slides for each antibody were obtained generally from any tissue.

Morphometric studies:

A light microscope (Leica ICC50 Wetzlar, Germany) was used for image analysis at the Histology Department, Faculty of Medicine, Sohag University. We analyzed ten non-overlapping high power fields (x400) for each case in all groups with Image J 1.51n software[13] for the following:

1- The percentage areas of P62, LC3 expression[14].

2- The PCNA labeling index was calculated as the number of positive cells/number of total cells counted in the field x100[15].

Statistical analysis:

Data were expressed as mean ± standard deviation. SPSS version 16 was used for Statistical analysis. Paired sample Student t-test was used to detect the significance of changes between the two groups. Data analysis was performed in a blinded fashion. Statistical significance was considered when $P < 0.05$[16].

RESULTS

Light microscopic studies:

H&E:

All control subgroups showed similar results. Examination of all animals in the control group and group II by H & E revealed typical spleen architecture with its two main components; white pulp which consisted of separated lymphoid follicles and surrounded by highly vascular matrix red pulp. A marginal zone was seen to demarcate between the two components. The white pulp-forming follicles had a peri-arteriolar lymphatic sheath which was represented as a dark area of lymphocytes around the central arteriole. Some follicles appeared with germinal centers. The germinal center contains acidophilic cells with vesicular nuclei. The red pulp consisted of a network of blood cell cords and numerous venous sinuses (Figures 1, 2).

On the other hand, meloxicam-treated groups (group III and group IV) showed disturbance in the architecture with atrophied lymphoid follicles and highly expanded red pulps seen in the red pulp. There were no apparent germinal centers or marginal zones in most of the follicles. Apoptotic cells with acidophilic cytoplasm and pyknotic nuclei were seen. Group IV showed more disturbances in architecture with more prominent degenerative changes (Figures 3, 4).

AuNPs administration attenuated meloxicam-induced changes; group V and group VI showed less disturbed architecture with fewer atrophied lymphoid follicles. Acidophilic cells with pyknotic nuclei were less seen than in meloxicam-treated groups (Figures 5, 6).

After stopping the injection of meloxicam with saline injection for 2 weeks, no improvement was observed; group VII and group VIII showed a structure more or less similar to that seen in meloxicam-treated groups of the corresponding time point in the form of disturbed splenic architecture with atrophied lymphoid follicles with apoptotic cells, highly expanded red pulps and dilated venous sinuses. Some vacuolated cells were seen. These changes were more obvious in group VIII, in addition to the presence of multiple megakaryocytes in the red pulp of this group (Figures 7, 8).

Silver nitrate:

In the control group, normal splenic architecture was observed (Figures 9 A - C). In AuNPs treated groups, it was observed that AuNPs were distributed homogenously in the spleen parenchyma, especially at the red pulp in macrophages (Figures 9 D - F). Meloxicam & AuNPs treated groups: the ratio of AuNPs accumulated in the macrophages after treatment with meloxicam was lower than that after treatment with AuNPs only. (Figures 9 G - I).

Immunohistochemistry:

1. PCNA antibody:

All control subgroups showed similar results. PCNA immunostained sections of groups I and II exhibited few positive cells in both white and red pulp. The positive reaction was observed as a nuclear brownish coloration (Figures 10 A, B). On the other hand, meloxicam-treated groups III and IV exhibited numerous positive cells in both white and red pulp (Figures 10 C, D). Meloxicam plus AuNPs treated groups (V and VI) showed a marked decrease in PCNA expression (Figures10 E, F). After meloxicam stoppage, (groups VII and VIII)

showed the persistence of increased positive cells (Figures 10 G, H).

2. LC3 antibody:

All control subgroups showed similar results. LC3 immunostained sections of groups I and II exhibited few positive cells in both white and red pulp. The positive reaction was observed as cytoplasmic brownish coloration (Figures 11 A, B). Meloxicam-treated groups (groups III and IV) exhibited numerous positive cells in both white and red pulp (Figures 11 C, D). Meloxicam plus AuNPs treated groups (groups V and VI) showed a marked decrease in LC3 expression compared to meloxicam-treated groups at the same time point (Figures 11 E, F). After meloxicam cessation, groups VII and VIII still showed increased positive cells (Figures 11 G, H).

3. p62 antibody:

All control subgroups showed similar results. Groups I and II exhibited few positive cells in both white and red pulp. The positive reaction was observed as cytoplasmic brownish coloration (Figures 12 A, B). On the other hand, meloxicam-treated groups (groups III and IV) exhibited numerous positive cells in both white and red pulp (Figures 12 C, D). Meloxicam plus AuNPs treated groups (groups V and VI) showed a marked decrease in LC3 expression compared to meloxicam-treated groups at the same time point (Figures 12 E, F). After meloxicam stoppage, (groups VII and VIII) still showed increased positive cells (Figures 12 G, H).

Statistical results:

In the PCNA index, LC3 and p62 expression area percentages, there was no significant difference between the control subgroups. Group II showed no significant difference compared to group I. The three parameters; PCNA index, LC3 and p62 expression area percentages showed a significant increase in all groups compared to the control. The mean of each parameter was significantly higher in group IV compared to that in group III. With AuNPs, the mean of each parameter was significantly decreased in groups V and VI compared to groups III and IV respectively. There was no significant difference between group VII and group VIII versus group III and group IV respectively (Figure 13 and Table 1).

Table 1: Mean PCNA labelling index, mean LC3 and mean p62 expression area percentages in all studied groups:

Groups	PCNA count labeling index	LC3 area percentage	*P62 area percentage*
Group I	5.93 ± 1.22	6.46 ± 1.13	7.56 ± 1.54
Group II	6.23 ± 1.45	7.00 ± 1.36	7.70 ± 1.44
Group III	38.29 ± 1.34*	22.93 ± 1.84*	27.96 ± 1.51*
Group IV	74.40 ± 3.19*#	32.66 ± 1.97*#	34.06 ± 2.01*#
Group V	29.24 ± 1.40*#	13.93 ± 3.66*#	13.93 ± 3.66*#
Group VI	38.66 ± 1.02*&	24.10 ± 1.748*&	25.76 ± 2.43*&
Group VII	38.83 ± 0.74*	23.16 ± 2.05*	27.13 ± 2.45*
Group VIII	73.56 ± 3.54*	33.50 ± 1.47*	35.26 ± 1.79*

* Signifiant versus control, # :significant versus group III,
& :significant versus group IV.

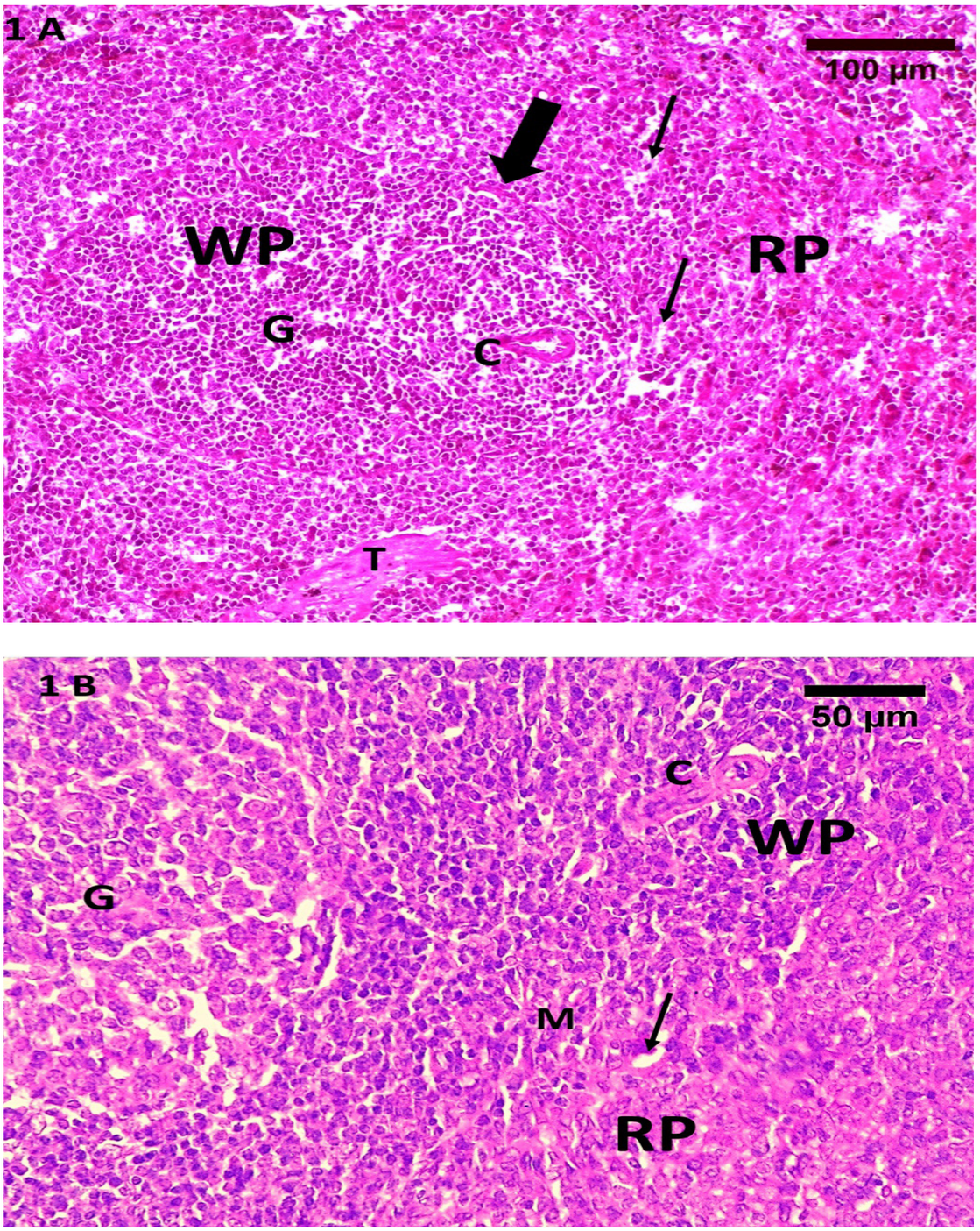

Figure 1: Photomicrographs of splenic sections of group I showing; lymphoid follicles (thick arrow) of the white pulp(WB) in a highly vascular matrix. red pulp (RB) with numerous venous sinuses (thin arrow) and thick trabeculae (T) . The white pulp consists of a peri-arteriolar lymphatic sheath around the central arteriole (C) and germinal center (G) contains acidophilic cells with vesicular nuclei), marginal zone (M). (H&E 1A,X200 with scale bar 100um ,1B X400 with scale bar 50 um).

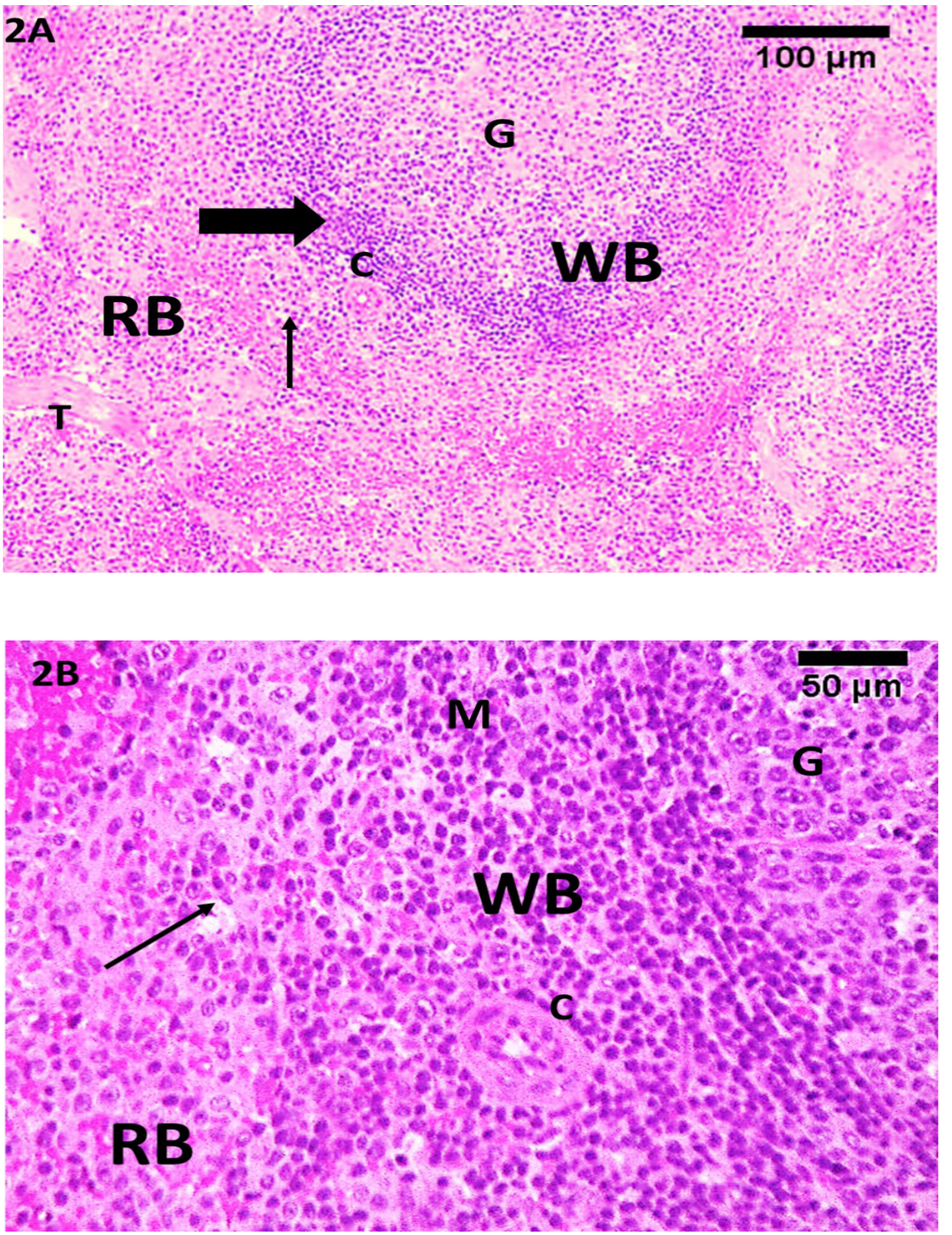

Figure 2: Photomicrographs of splenic sections of group II showing lymphoid follicles (thick arrow) of the white pulp (WP) in a highly vascular matrix, red pulp (RP) with numerous venous sinuses (thin arrow) and thick trabeculae (T). The white pulp consists of a peri-arteriolar lymphatic sheath around the central arteriole (C) and germinal center (G contains acidophilic cells with vesicular nuclei and well-distinct marginal zone (M). (H&E,2A,X200 with scale bar 100um, 2B X400 with scale bar 50 um).

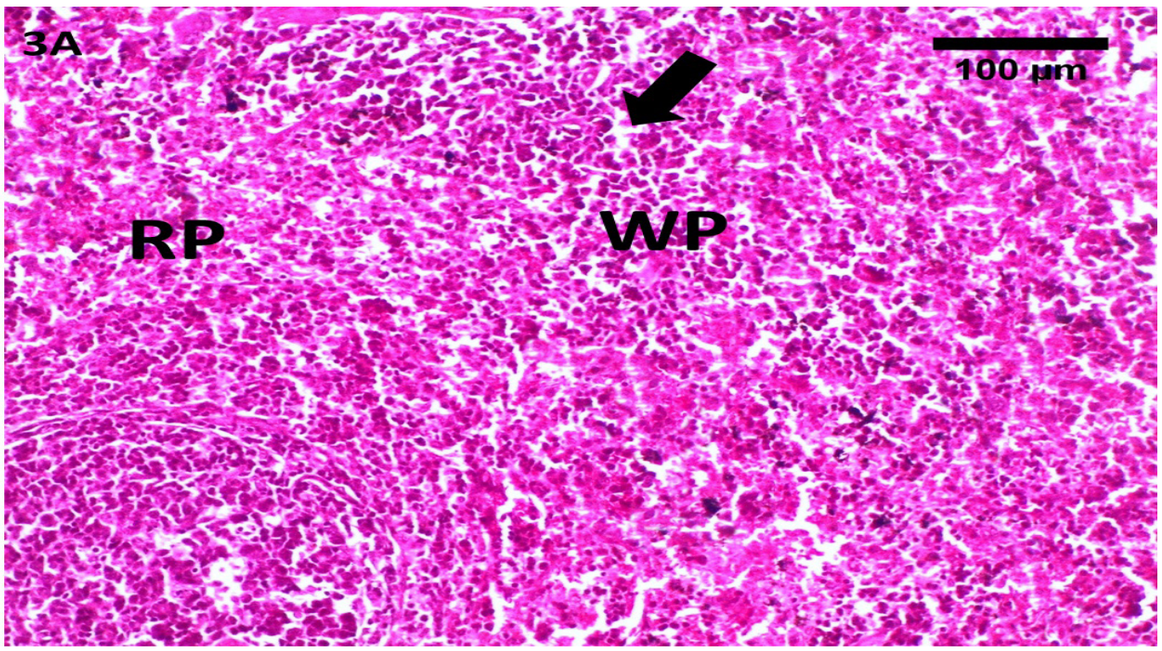

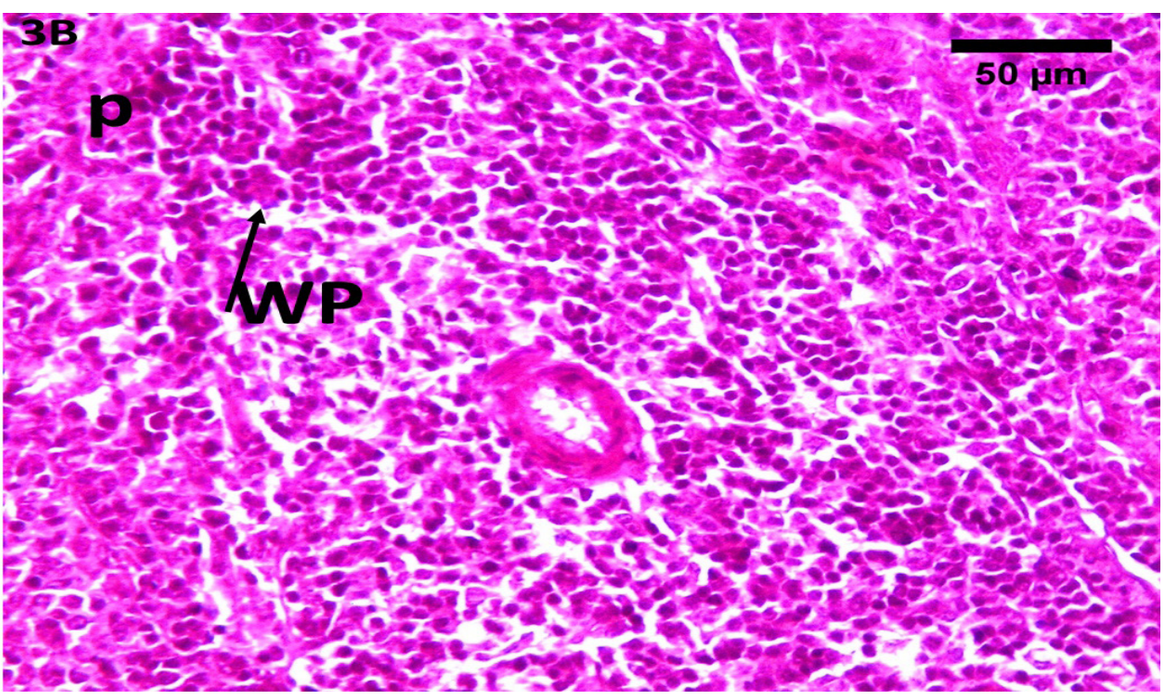

Figure 3: Photomicrographs of splenic sections of group III showing: some disturbance in the architecture with atrophied lymphoid follicles (thick arrow) in white pulp (WP) with pyknotic nuclei (P) and expanded red pulp (RP) with dilated venous sinuses (thin arrow) (H&E,3A,X200 with scale bar 100um ,3B X400 with scale bar 50 um).

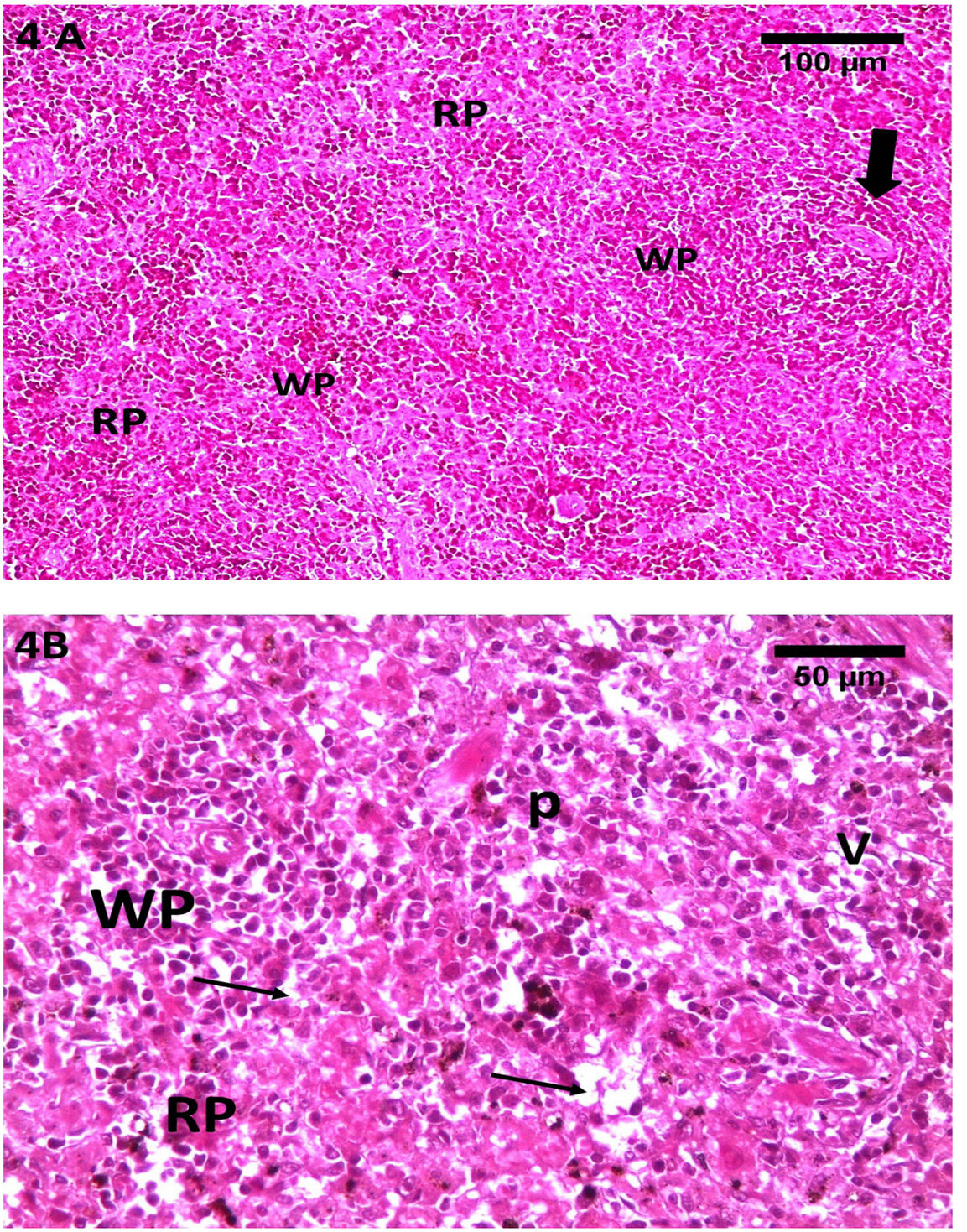

Figure 4: Photomicrographs of splenic sections of group IV showing more disturbance in architecture with marked atrophied lymphoid follicles (thick arrow)in white pulp (WP)with most Splenic lymphocytes have pyknotic nuclei (P) and highly expanded red pulp (RP) with dilated venous sinuses (thin arrow) . Vacuolated cells (V) are seen in the red pulp (H&E, 4A X200 with scale bar 100um ,4B X400 with scale bar 50 um).

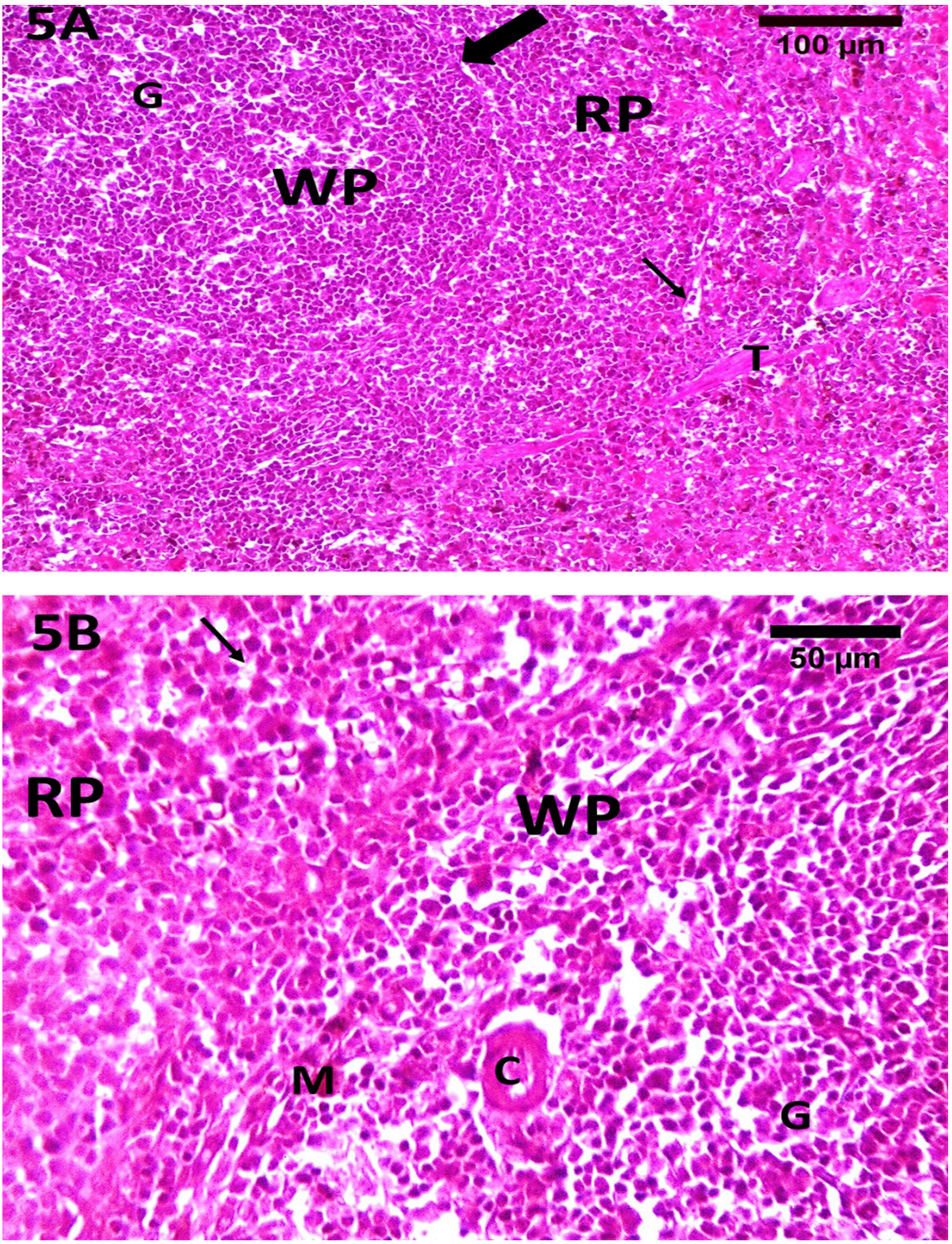

Figure 5: Photomicrographs of splenic sections of group V showing more or less normal splenic architecture with lymphoid follicles (thick arrow) in white pulp(WP) have germinal center (G) and central arteriole (C) , red pulp (RP). Venous sinuses (thin arrow) trabeculae(T). Marginal zone (M) (H&E, 5A X200 with scale bar 100um, 5B X400 with scale bar 50 um).

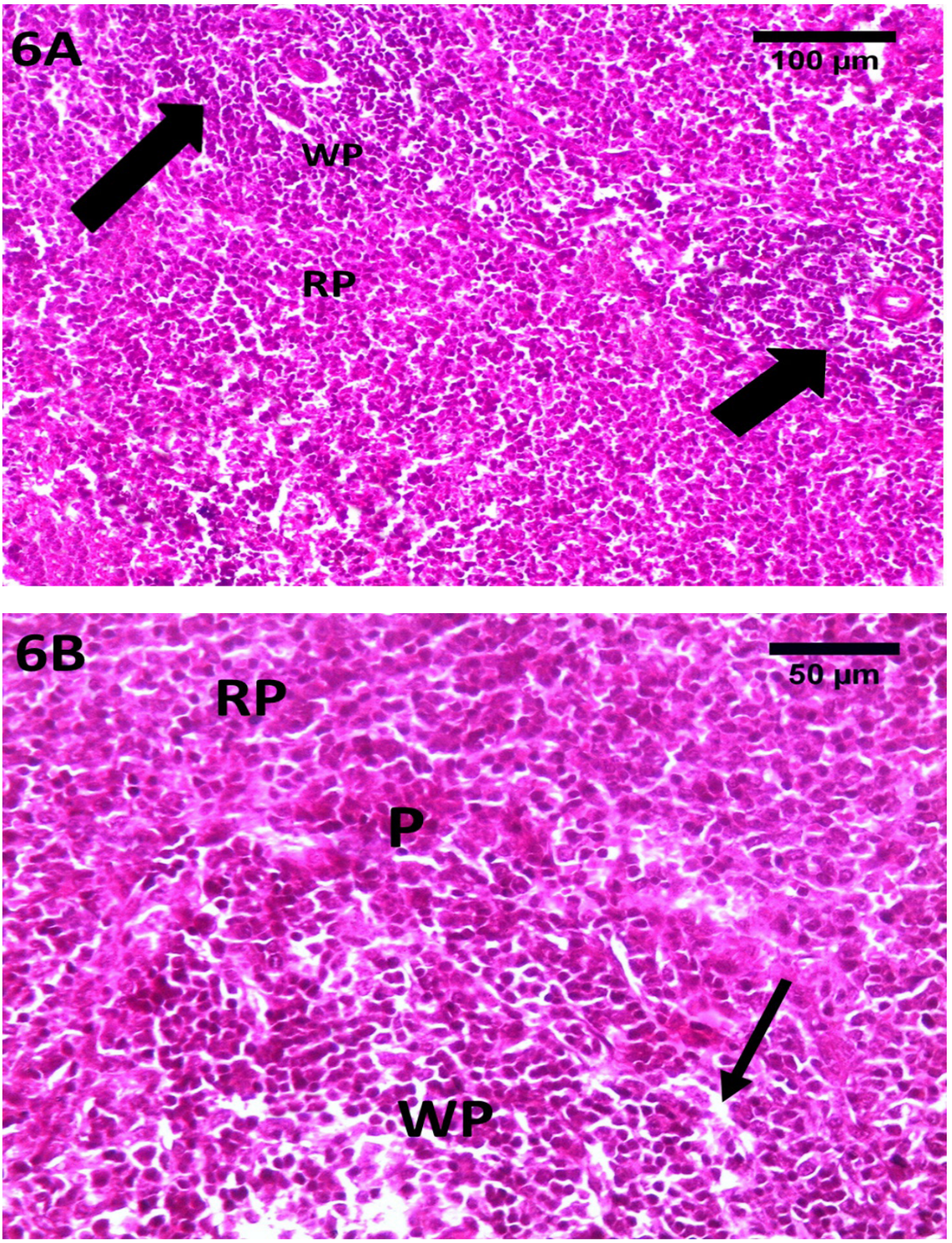

Figure 6: Photomicrographs of splenic sections of group VI showing less disturbance in the architecture with atrophied lymphoid follicles (thick arrow) in white pulp (WP),less expanded red pulp (RP). Note few splenic lymphocytes in the atrophied follicle have acidophilic cytoplasm and pyknotic nuclei (P) and few dilated sinuses (thin arrow) in the red pulp (H&E, 6AX200 with scale bar 100um ,6B X400 with scale bar 50 um).

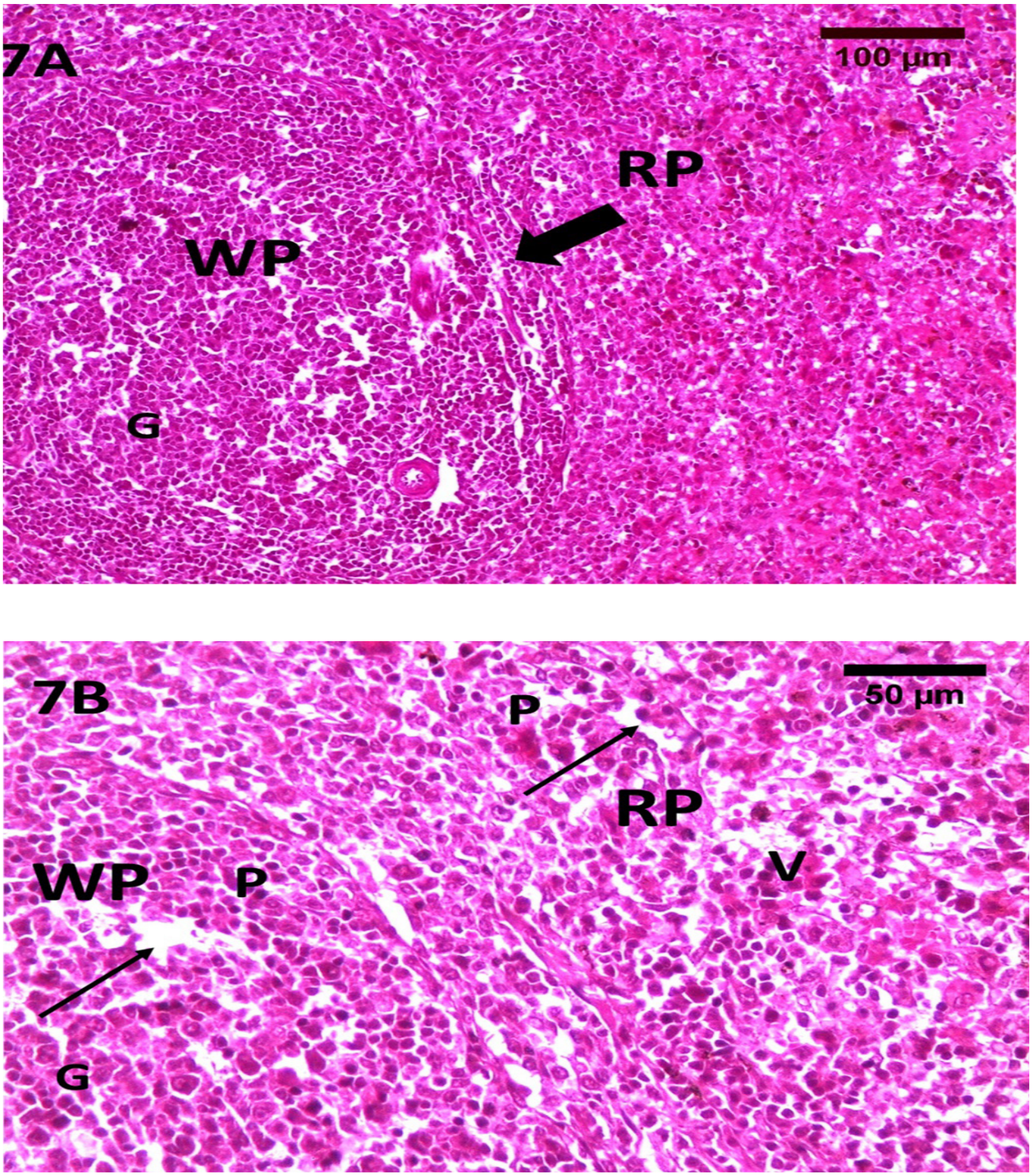

Figure 7: Photomicrographs of splenic sections of group VII showing disturbed architecture in lmphoid follicles (thick arrow) in white pulp(WP) with germinal center (G) , red pulps(RP) with dilated sinuses (thin arrow).with some vacuolated cells (V). some Splenic lymphocytes have pyknotic nuclei(P). (H&E 7AX200 with scale bar 100um,7B X400 with scale bar 50 um).

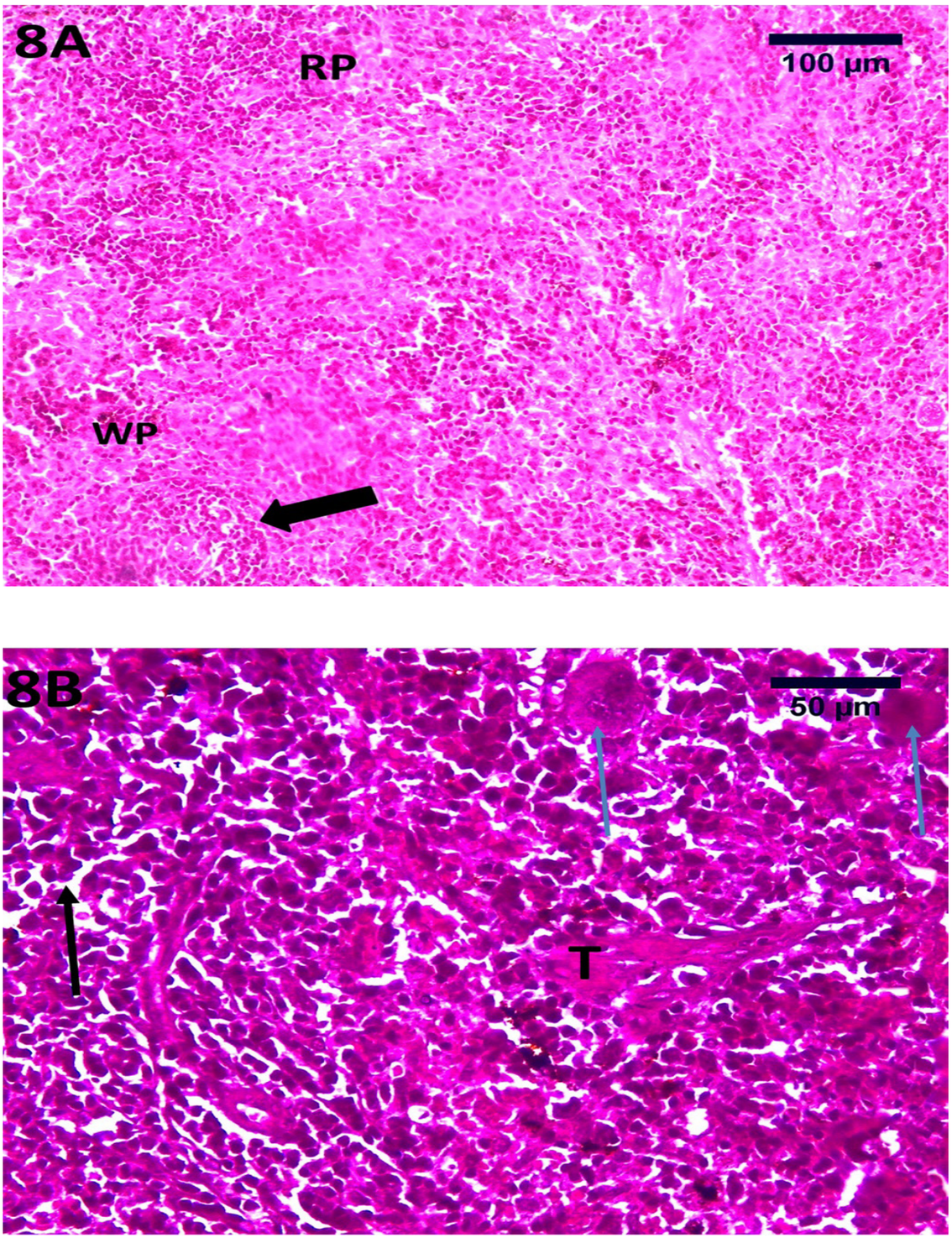

Figure 8: Photomicrographs of splenic sections of group VIII showing highly disturbed splenic architecture, white pulp (WP) with atrophied lymphoid follicles (thick arrow) , and highly expanded red pulps (RP).Most cells have pyknotic nuclei in both red and white pulp. Dilated sinuses (thin arrow). Multiple megakaryocytes (blue arrow) are seen in red pulp the fibrous trabeculae (T) (H&E 8AX200 with scale bar 100um ,8B X400 with scale bar 50 um).

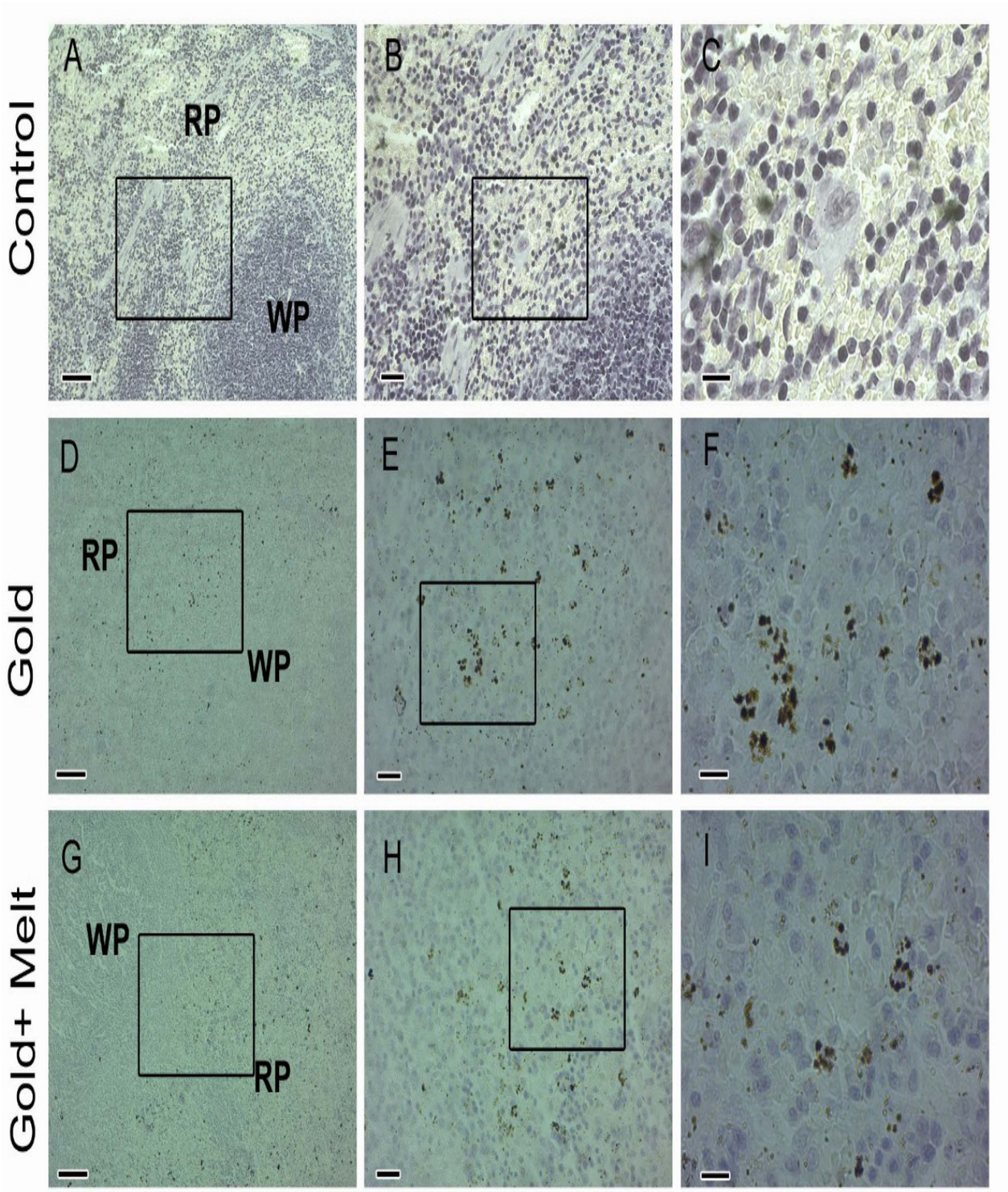

Figure 9: Photomicrographs of splenic sections stained with silver enhancer stain to enhance localization of AuNPs. (A-C); The spleen of control animals without any treatment is showing normal white and red pulp. (D-F); the spleen of animals from group II after treatment with AuNPs only is showing macrophages filled with AuNPs. (G-I); the spleen of the treated animals with AuNPs and meloxicam (groups V, VI) is showing accumulation of the AuNPs in the macrophages but with a low ratio compared with AuNPs treatment only. Scale bar: A, D, G = 50 μm; B, E, H = 10 μm; C, F, I = 5 μm.

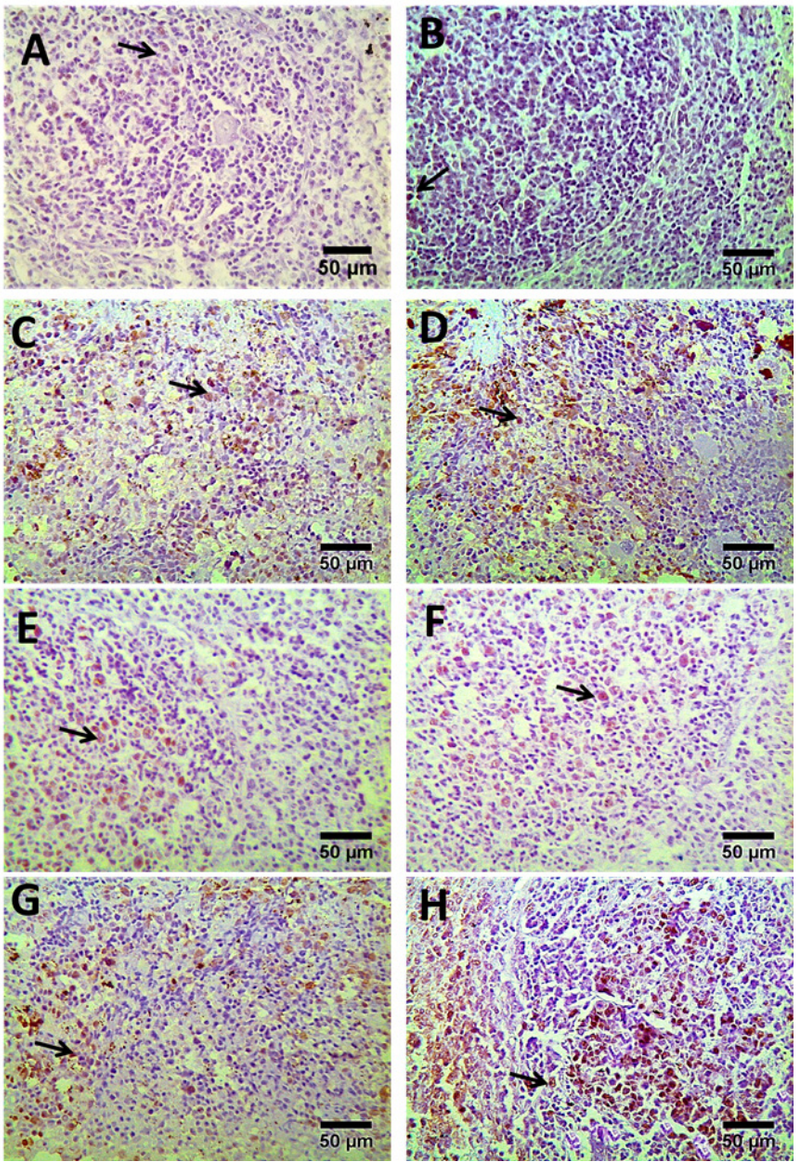

Figure 10: Photomicrographs of spleen sections immunostained with PCNA antibody. (A, B) showing few positively stained cells (arrow) appear as nuclear brownish coloration in group I and II which is increased in group III (C) and markedly increased in group IV (D) then decreased again in group V and VI (E,F) . Some positive cells are seen in group VII (G) and many positive cells in group VIII (H).) PCNA antibody ×400, scale bar =50 um).

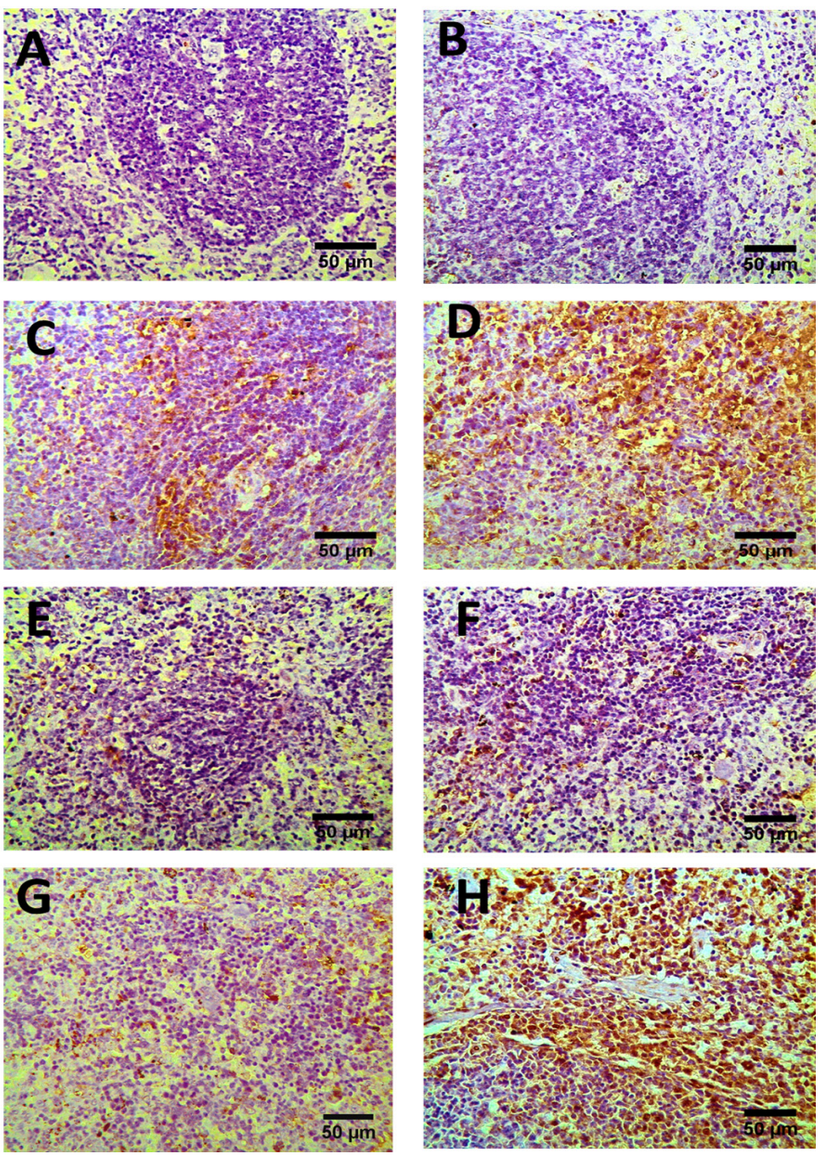

Figure 11: Photomicrographs of spleen sections immunostained with LC3 antibody. (A, B) showing few positively stained cells appear as cytoplasmic brownish coloration in group I and II which is increased in group III (C) and markedly increased in group IV (D)then decreased again in group V and VI (E,F) . Some positive cells are seen in group VII (G) and many positive cells are seen in group VIII (H). (LC3 antibody ×400, scale bar =50 um).

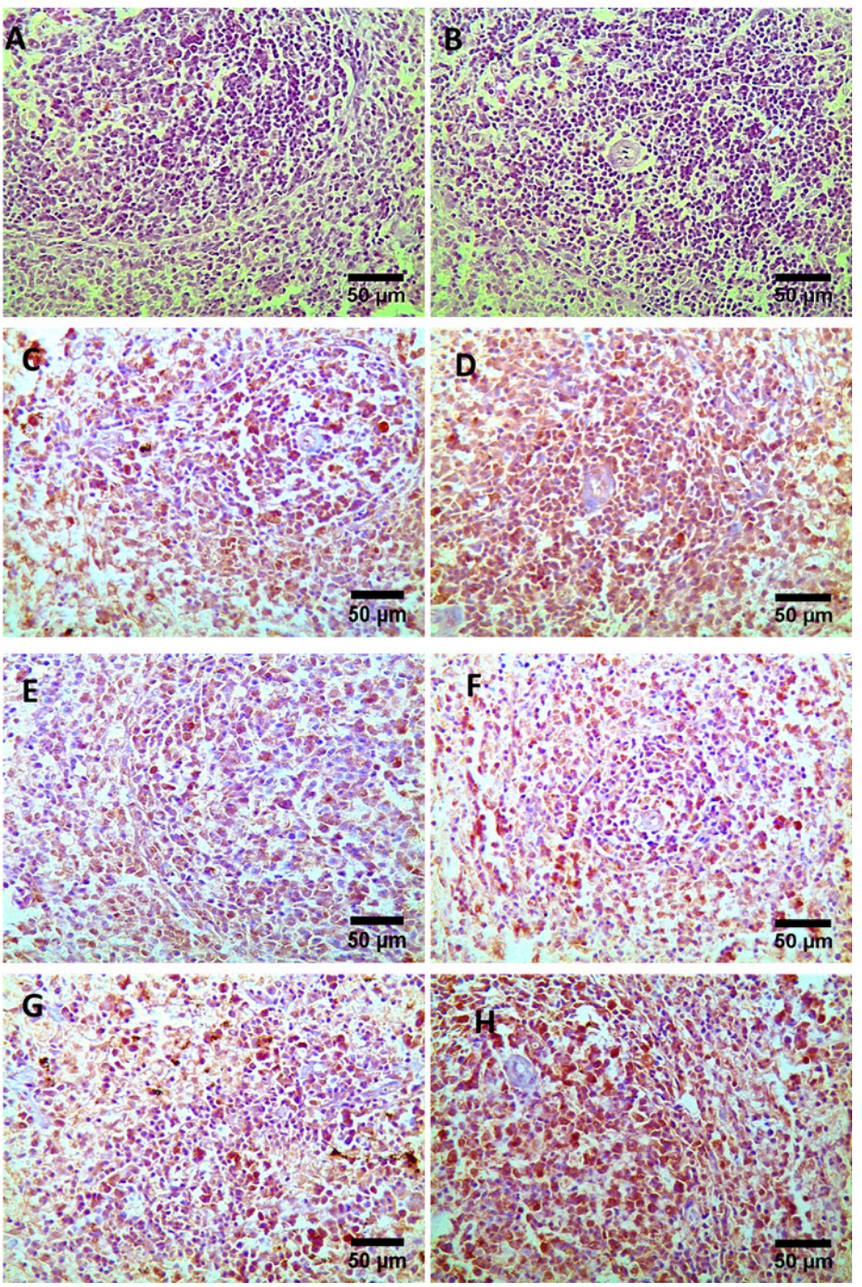

Figure 12: Photomicrographs of spleen sections immunostained with p62 antibody. (A, B) showing few positively stained cells seen as cytoplasmic brownish coloration in group I and II which is increased in group III (C) and markedly increased in group IV (D)then decreased again in group V and VI (E,F) . Some positive cells are seen in group VII (G) and many positive cells are seen in group VIII(H). (p62 antibody ×400, scale bar =50 um).

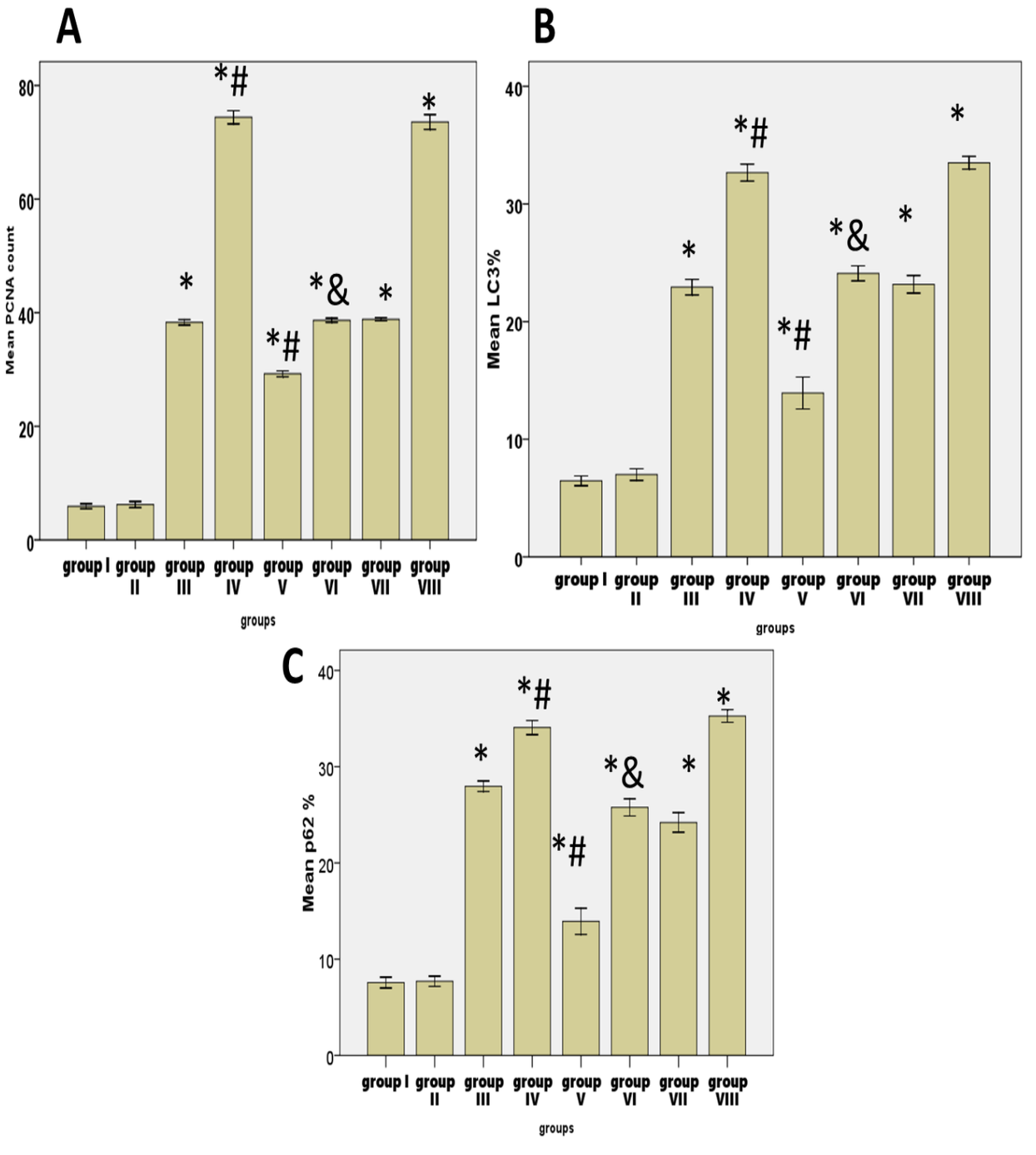

Figure 13: Histogram representing: A) mean PCNA labeling index, B) mean LC3 expression area percentages and C) mean p62 expression area percentages in all studied groups. *significant versus control, #: significant versus group III, & significant versus group IV.

DISCUSSION

Meloxicam is one of the NSAIDs which is commonly used for the treatment of rheumatic diseases[17]. Meloxicam is a selective inhibitor of COX2 which decreases prostaglandin E2 and leads to an increase in free radicals within the cell[18]. With the increased awareness of the importance of nanotechnology in medicine, the applications of AuNPs have increased as an antioxidant[19].

In our study, we assess the possible therapeutic effect of AuNPs (50 ul) on meloxicam-induced splenic toxicity in a dose of (15 mg/kg) at different time points.

In our study, the AuNPs received group had a histological appearance more or less similar to the control group. This could be attributed to the use of a nontoxic dose of AuNPs in our study. In addition, we used the average diameter (10 nm) of AuNPs which is not retained in the cell and easily excreted. Thus, they did not induce cellular toxicity. In agreement with our findings, a previous study used AuNPs in different doses (50, 100 and 150 UI) orally and proved that they were nontoxic at 50 ul[20]. However, Tedesco *et al.*[21] disagreed with our results and proved that 10 nm diameter AuNPs were toxic because they produced membrane lipid peroxidation via direct contact with membranes, but this was in the blue mussel, Mytilus edulis. AuNPs can exhibit a cytotoxic profile when the size is below 2 nm[22]. The smallest nanoparticles showed more deleterious effects, confirmed by their location inside the cell nucleus and the higher DNA damage[23].

We used silver nitrate to demonstrate the localization of AuNPs in the spleen. Silver ions adhere to the catalytic surface of the gold nanoparticles. Then, the gold nanocrystal induces the reduction of the silver ions into atoms releasing electrons around it. This results in increasing the size of the nanocrystals, enabling their visualization under the light microscope[11]. AuNPs are favorably used in liver and spleen diseases. AuNPs are accumulated in the spleen and liver, due to the rich blood supply of these organs and the presence of numerous resident macrophages. AuNPs are engulfed by the reticuloendothelial system[7].

With immunohistochemistry, we used the PCNA antibody which is the most important marker used to assess cell proliferation. We found that control groups had few positive cells. Also, we found in the control that P62 and LC3 were positive in a few cells due to preserved autophagy functions.

In the groups receiving meloxicam, many histological changes were observed. The changes were more prominent in the longer duration of meloxicam administration (group IV) in the form of disturbance in architecture with atrophied lymphoid follicles, highly expanded red pulps with dilated venous sinuses and apoptotic lymphocytes in the atrophied follicle. There was no apparent germinal center or marginal zone in most of the follicles. In agreement with our findings, Baraaj[24] reported that meloxicam treatment for seven weeks induced degenerative histological changes in the spleen; both in white and red pulps in the form of the presence of apoptotic cells and necrotic areas. In addition, Burukoglu *et al.*[1] found necrosis and apoptosis in liver cells with meloxicam toxicity. These degenerative changes were due to meloxicam metabolites which caused oxidative stress with mitochondrial dysfunction and then apoptosis. Moreover, the decreased prostaglandin which had anti-apoptotic mitochondrial activity triggered apoptosis[2]. Another explanation for the mechanism of apoptosis by meloxicam was its inhibitory effect on COX-2 which had an antiapoptotic function. Pyknosis was due to a disturbance in the DNA of the splenic cells caused by the drug[25].

In contrast to our study, Hassan *et al.*[26] used meloxicam as a renoprotective agent against doxorubicin toxicity. Edfawy *et al.*[27] reported the protective role of meloxicam against carbon tetrachloride-induced liver damage. This could be explained by the anti-inflammatory property of meloxicam. It decreases inflammatory prostaglandin E2, inflammatory cytokines as interleukin 6 and tumor necrosis factor.

By immunostaining, there was a significant increase in PCNA immunoexpression in meloxicam-treated groups as compared to the control group with significantly higher expression in 2 months than seen in the 2 weeks group. Similar results were reported in splenic toxicity and hepatotoxicity by Al-Medhtiy *et al.*[28]. PCNA increase is an indicator of increased cellular proliferation. PCNA is a nuclear protein that uses the polymerase S addition protein[29]. Al-Medhtiy *et al.*[28] explained that this increase in cell proliferation was to compensate for cell injury. PCNA holds DNA polymerase epsilon which is involved in DNA repair and synthesis of damaged DNA strands after repetitive cell damage[30]. Zhang *et al.*[30] reported that the increased PCNA expression in diabetic liver was associated with autophagy dysfunction due to cell damage resulting from endoplasmic reticulum stress.

The autophagic markers p62 and LC3 immunoexpression increased in meloxicam-treated groups as compared to the control group with significantly more expression in 2 months than seen in the 2 weeks group indicating marked autophagy suppression in this group.

In agreement with our results, Liao *et al.*[31] study observed the accumulation of autophagosomes for degradation. Zhao *et al.*[32] reported that mercury-induced toxicity significantly up-regulated LC3 and p62 immunoexpression in the spleen due to impairment of autophagic flux leading to the accumulation of these proteins. Xu *et al.*[33] reported impairment of autophagy with increased LC3 and p62 immunoexpression in lung macrophages in human cases of paraquat-induced pulmonary toxicity. LC3 enables autophagosomes to bind autophagic substrates including p62 with ubiquitinated cargo which ends with the fusion of autophagic vacuoles with lysosomes and the recycling of contents[34]. Ca2+ signals stimulate autophagy via activation of the phosphatase calcineurin. Autophagic cell death can occur in case of oxidative stress-induced mitochondrial Ca2+ disturbance. Inhibition of cytosolic Ca2+ signals could suppress the fusion of autophagic vacuoles with lysosomes which leads to the accumulation of LC3 and p62[32]. Reactive oxygen species participate in triggering the conversion of LC3-I into LC3-II and the subsequent triggering of autophagy but end with the accumulation of autophagic vacuoles due to impairment of autophagic flux and lysosomal fusion[35]. Moreover, the decrease in lysosomal proteolytic activity affected the autophagic vacuole degradation leading to P62 and LC3 accumulation[36].

In contrast to our results, a previous study reported that a COX-2 inhibitor decreased the LC3 level. They explained that COX-2 controls the relation between endoplasmic stress and autophagy[37].

Our results demonstrated a marked reduction in the expression of P62 and LC3 in meloxicam plus AuNPs groups. These occur due to the upregulation of autophagy by increasing the pre-autophagosomal structure and decreased SQSTM1/P62 and LC3 within the splenic lymphocytes[38]. In many cases of cellular stress, autophagy cross-talks with apoptosis as both processes are very important for cellular homeostasis[39].

The groups that received meloxicam plus AuNPs (groups V, VI) showed improvement in the degenerative histological changes induced by meloxicam; regular organization of white and red pulp and decreased apoptotic cells were observed. Also, PCNA immunoexpression was downregulated. In agreement with our results, a previous study reported that AuNPs could also scavenge free radicals & oxidative stress as they decreased lipid peroxidation and increased glutathione in Schistosoma Mansoni splenomegaly[40].

Similar to our results, Boomi *et al.*[5] reported that AuNPs have potent free radical scavenging activity in wound healing. This may be due to their ability to neutralize the free radicals via the donation of electrons or hydrogen ions.

Reshi *et al.*[20] indicated that AuNPs could improve hepatic & renal toxicity induced by acetaminophen as AuNPs could restore cellular structures by maintaining cell permeability. Also, Abdo *et al.*[7] used AuNPs against carbon tetrachloride-induced liver injury. They explained that AuNPs could selectively enter degenerated cells and counteract apoptotic enzymes. In a previous study, de Carvalho *et al.*[41] used AuNPs to improve the inflammation & oxidative stress in a rat model of alcohol-methamphetamine-induced liver injury. They found that AuNPs had an anti-inflammatory effect through the inhibition of nitrite and pro-inflammatory cytokines in macrophages. The reduction of PCNA expression with AuNPs in our results was due to reduced repeated cell damage and subsequent DNA repair induced by meloxicam toxicity.

In contrast to our results, a previous study reported that AuNPs caused significant degenerative changes in the spleen from the second day of administration and persisted till day 8 but with diameters of (20 nm) and (50 nm) nanoparticles[42]. Doudi and Setorki[43] indicated that AuNPS were toxic and caused vacuolations in hepatocytes and hepatocellular degeneration. The hepatotoxicity is caused by the accumulation and deposition of AuNPs in the liver which induced oxidative stress. Ibrahim *et al.*[42] explained that the size of AuNPs determines their toxic effects.

By silver nitrate staining of these groups, there was observed accumulation of AuNPs in Macrophages but with less ratio compared with AuNPs only treated group. This might be due to the use of AuNPs to counteract meloxicam toxicity. AuNPs induce recovery of cell damage via the down-regulation of macrophages. This explained the decrease in macrophages in the meloxicam &

AuNPs treated group compared to the AuNPs-only treated group[7].

In the meloxicam & AuNPs treated groups, our results revealed that AuNPs downregulated LC3 and p62 expression which were overexpressed by meloxicam due to activation of autophagy. Similar to our results, Zhang *et al.*[44] reported that AuNPs could significantly induce bone regeneration in ectopic models via downregulation of p62 due to stimulation of autophagy.

In contrast, other studies reported that AuNPs could modulate autophagy by suppressing autophagic flux[6]. This discrepancy could be explained by the difference in shape and size of the used nanoparticles.

In groups VII and VIII, we found no attenuation of degenerative histological changes induced by meloxicam or downregulation in the immunoexpression of autophagic markers which were upregulated in meloxicam treated groups. Ebaid *et al.*[45] suggested that this might be due to the immune system exhibiting a delayed response to the drug. In agreement with our results, Ahmad *et al.*[46] reported that meloxicam in a dose of (3 mg\kg) caused marked persistent degeneration of hepatocytes and severe dilatation of the central vein. They explained that after the cessation of therapy, no improvement was observed due to the severely damaged cells. This finding confirmed the alleviating role caused by AuNPs against meloxicam toxicity.

In addition, we observed the presence of numerous megakaryocytes in the spleen sections of group VIII. Machlus and Italiano[47] explained that COX-2 inhibition delays bone marrow megakaryopoiesis promoting compensatory splenic megakaryocyte hyperplasia. Megakaryocytes appeared in this group not before because the life cycle of the cell needs several days to appear.

CONCLUSION

Our study revealed obvious time dependent degenerative changes in the spleen after meloxicam injection. However, AuNPs caused improvement in these changes. So, AuNPs are considered to have a therapeutic effect against the toxic effects of meloxicam in the spleen which may be due to their free radical scavenging and antioxidant activities, in addition to the activation of autophagy.

Abbreviations: NSAID; non-steroidal anti-inflammatory drug, COX-2; cyclooxygenase 2, AuNPs; gold nanoparticles.

CONFLICT OF INTEREST

There is no potential conflict of interest among the authors.

REFEREANCES

1. Burukoglu, D., Baycu, C., Taplamacioglu, F., Sahin, E. and Bektur, E. Effects of nonsteroidal anti-inflammatory meloxicam on stomach, kidney and liver of rats. Toxicology and industrial health. 2016; 32(6): p. 980986-.

2. Mohammed, N.M., El-Drieny, E., Ibrahim, S., Al-agory, M. and Gheth, E.M. Histopathological Changes in liver tissue induced by meloxicam in male mice. International Journal of Pharmacy & Life Sciences. 2019; 10(1): p. 60596063-.

3. Combes, F., Meyer, E. and Sanders, N.N. Immune cells as tumor drug delivery vehicles. Journal of Controlled Release. 2020; 327: p. 7087-.

4. Sibuyi, N.R.S., Moabelo, K.L., Fadaka, A.O., Meyer, S., Onani, M.O., Madiehe, A.M. and Meyer, M. Multifunctional gold nanoparticles for improved diagnostic and therapeutic applications: a review. Nanoscale Research Letters. 2021; 16(1): p. 127-.

5. Boomi, P., Ganesan, R., Poorani, G.P., Jegatheeswaran, S., Balakumar, C., Prabu, H.G., Anand, K., Prabhu, N.M., Jeyakanthan, J. and Saravanan, M. Phyto-engineered gold nanoparticles (AuNPs) with potential antibacterial, antioxidant and wound healing activities under in vitro and in vivo conditions. International journal of nanomedicine. 2020; 15: p. 7553.

6. Zhou, H., Gong, X., Lin, H., Chen, H., Huang, D., Li, D., Shan, H. and Gao, J. Gold nanoparticles impair autophagy flux through shape-dependent endocytosis and lysosomal dysfunction. Journal of Materials Chemistry B. 2018; 6: p. 81278136-.

7. Abdo, F.K., Ahmed, F.E., Alazouny, Z. and Hassan, S. Silymarin versus gold nanoparticles efficacy in ameliorating CCl4-induced liver fibrosis in adult male Albino rats: A histological and immunohistochemical study. British Journal of Science. 2016; 13(2): p. 1323-.

8. Abdelhalim, M. and Mady, M. Liver uptake of gold nanoparticles after intraperitoneal administration in vivo: A fluorescence study. Lipids in health and disease. 2011; 10: p. 195.

9. Levin-Arama, M., Abraham, L., Waner, T., Harmelin, A., Steinberg, D., Lahav, T. and Harlev, M. Subcutaneous Compared with Intraperitoneal Ketamine-Xylazine for Anesthesia of Mice. Journal of the American Association for Laboratory Animal Science: JAALAS. 2016; 55: p. 794800-.

10. Bancroft, J.D. Histochemical techniques. 2013: Butterworth-Heinemann.

11. Liu, R., Zhang, Y., Zhang, S., Qiu, W. and Gao, Y. Silver enhancement of gold nanoparticles for biosensing: from qualitative to quantitative. Applied Spectroscopy Reviews. 2014; 49(2): p. 121138-.

12. Hussein, G., Nakamura, M., Zhao, Q., Iguchi, T., Goto, H., Sankawa, U. and Watanabe, H. Antihypertensive and neuroprotective effects of astaxanthin in experimental animals. Biological & pharmaceutical bulletin. 2005; 28(1): p. 4752-.

13. Abdelmegeed, M.A., Choi, Y., Godlewski, G., Ha, S.-K., Banerjee, A., Jang, S. and Song, B.-J. Cytochrome P4502-E1 promotes fast food-mediated hepatic fibrosis. Scientific reports. 2017; 7(1): p. 112-.

14. Martinet, W., Schrijvers, D.M., Timmermans, J.P., Bult, H. and De Meyer, G.R. Immunohistochemical analysis of macroautophagy: recommendations and limitations. Autophagy. 2013; 9(3): p. 386402-.

15. Chaloob, M., Ali, H., Qasim, B. and Mohammed, A. Immunohistochemical Expression of Ki-67, PCNA and CD34 in Astrocytomas: A Clinicopathological Study. Oman medical journal. 2012; 27: p. 36874-.

16. Levesque, R. SPSS programming and data management. 4th ed. A guide for SPSS and SAS Users. 2007, chicago: SPSS Inc.3.

17. EL-Zogheby, R.R. and Abd-El-Azem, M. CYTOGENETIC AND BIOCHEMICAL CHANGES OF MELOXICAM IN ALBINO RATS. in Proceedings of the 5th Scientific Conference of Animal Wealth Research in the Middle East and North Africa, Faculty of Agriculture, Cairo University, Giza, Egypt, 13- October 2012. 2012. Massive Conferences and Trade Fairs.

18. Khan, A.M. and Rampal, S. Effects of repeated oral administration of pazufloxacin mesylate and meloxicam on the antioxidant status in rabbits. Journal of the American Association for Laboratory Animal Science. 2014; 53(4): p. 399403-.

19. Kumar, P. and Roy, I. Applications of gold nanoparticles in clinical medicine. Int J Pharm Pharm Sci. 2016; 8(7): p. 116-.

20. Reshi, M.S., Shrivastava, S., Jaswal, A., Sinha, N., Uthra, C. and Shukla, S. Gold nanoparticles ameliorate acetaminophen induced hepato-renal injury in rats. Experimental and Toxicologic Pathology. 2017; 69(4): p. 231240-.

21. Tedesco, S., Doyle, H., Blasco, J., Redmond, G. and Sheehan, D. Exposure of the blue mussel, Mytilus edulis, to gold nanoparticles and the pro-oxidant menadione. Comparative Biochemistry and Physiology Part C: Toxicology & Pharmacology. 2010; 151(2): p. 167174-.

22. Schmid, G., Kreyling, W.G. and Simon, U. Toxic effects and biodistribution of ultrasmall gold nanoparticles. Archives of toxicology. 2017; 91(9): p. 30113037-.

23. Lopez-Chaves, C., Soto-Alvaredo, J., Montes-Bayon, M., Bettmer, J., Llopis, J. and Sanchez-Gonzalez, C. Gold nanoparticles: Distribution, bioaccumulation and toxicity. In vitro and in vivo studies. Nanomedicine : nanotechnology, biology and medicine. 2018; 14(1): p. 112-.

24. Baraaj, A. Hematological and Histpathological Changes in Spleen of Male Albino Rats(Rattus norvegicus) Treated with Meloxicam. 2021: p. 13711374-.

25. Kasper, H.-U., Konze, E., Dienes, H.P., Stippel, D.L., Schirmacher, P. and Kern, M. COX-2 expression and effects of COX-2 inhibition in colorectal carcinomas and their liver metastases. Anticancer research. 2010; 30(6): p. 20172023-.

26. Hassan, M.H., Ghobara, M. and Abd-Allah, G.M. Modulator effects of meloxicam against doxorubicin-induced nephrotoxicity in mice. Journal of biochemical and molecular toxicology. 2014; 28(8): p. 337346-.

27. Edfawy, M., Hassan, M.H., Mansour, A., Hamed, A.-A. and Amin, H.A.A. Meloxicam Modulates Oxidative Stress Status, Inhibits Prostaglandin E2

and Abrogates Apoptosis in Carbon Tetrachloride–Induced Rat Hepatic Injury. International journal of toxicology. 2012; 31(3): p. 276286-.

28. Al-Medhtiy, M., Abduljabbar, A., Shareef, S., Abdel Aziz Ibrahim, I., Alzahrani, A. and Abdulla, M. Histopathological Evaluation of Annona muricata in TAA-Induced Liver Injury in Rats. Processes. 2022; 10: p. 1613.

29. Mathews, M.B. The proliferating cell nuclear antigen, PCNA, a cell growth-regulated DNA replication factor, in Growth control during cell aging. 2020, CRC Press. p. 89120-12089-.

30. Zhang, Q., Li, Y., Liang, T., Lu, X., Zhang, C., Liu, X., Jiang, X., Martin, R.C., Cheng, M. and Cai, L. ER stress and autophagy dysfunction contribute to fatty liver in diabetic mice. International journal of biological sciences. 2015; 11(5): p. 55968-.

31. Liao, W., Wang, Z., Fu, Z., Ma, H., Jiang, M., Xu, A. and Zhang, W. p62/SQSTM1 protects against cisplatin-induced oxidative stress in kidneys by mediating the cross talk between autophagy and the Keap1-Nrf2 signalling pathway. Free Radical Research. 2019; 53(7): p. 800814-.

32. Zhao, G., Qi, L., Wang, Y., Li, X., Li, Q., Tang, X., Wang, X. and Wu, C. Antagonizing effects of curcumin against mercury-induced autophagic death and trace elements disorder by regulating PI3K/AKT and Nrf2 pathway in the spleen. Ecotoxicology and Environmental Safety. 2021; 222: p. 112529.

33. Xu, G., Wang, X., Yu, H., Wang, C., Liu, Y., Zhao, R. and Zhang, G. Beclin 1, LC3 and p62 expression in paraquat-induced pulmonary fibrosis. Human & Experimental Toxicology. 2019; 38(7): p. 794802-.

34. Hayashi, K., Suzuki, Y., Fujimoto, C. and Kanzaki, S. Molecular Mechanisms and Biological Functions of Autophagy for Genetics of Hearing Impairment. Genes. 2020; 11(11): p. 1331.

35. Wei, S., Qiu, T., Yao, X., Wang, N., Jiang, L., Jia, X., Tao, Y., Wang, Z., Pei, P. and Zhang, J. Arsenic induces pancreatic dysfunction and ferroptosis via mitochondrial ROS-autophagy-lysosomal pathway. Journal of hazardous materials. 2020; 384: p. 121390.

36. Inami, Y., Yamashina, S., Izumi, K., Ueno, T., Tanida, I., Ikejima, K. and Watanabe, S. Hepatic steatosis inhibits autophagic proteolysis via impairment of autophagosomal acidification and cathepsin expression. Biochemical and biophysical research communications. 2011; 412(4): p. 618-625.

37. Chen, P., Geng, N., Zhou, D., Zhu, Y., Xu, Y., Liu, K., Liu, Y. and Liu, J. The regulatory role of COX-2 in the interaction between Cr(VI)-induced endoplasmic reticulum stress and autophagy in DF-1 cells. Ecotoxicology and Environmental Safety. 2019; 170: p. 112119-.

38. Tsai, S.Y., Chung, P.C., Owaga, E.E., Tsai, I.J., Wang, P.Y., Tsai, J.I., Yeh, T.S. and Hsieh, R.H. Alpha-mangostin from mangosteen (Garcinia mangostana Linn.) pericarp extract reduces high fat-diet induced hepatic steatosis in rats by regulating mitochondria function and apoptosis. Nutrition & metabolism. 2016; 13: p. 88.

39. Yan, S., Huda, N., Khambu, B. and Yin, X.-M. Relevance of autophagy to fatty liver diseases and potential therapeutic applications. Amino acids. 2017; 49(12): p. 19651979-.

40. Dkhil, M.A., Khalil, M.F., Diab, M.S., Bauomy, A.A. and Al-Quraishy, S. Effect of gold nanoparticles on mice splenomegaly induced by schistosomiasis mansoni. Saudi Journal of Biological Sciences. 2017; 24(6): p. 14181423-.

41. de Carvalho, T.G., Garcia, V.B., de Araújo, A.A., da Silva Gasparotto, L.H., Silva, H., Guerra, G.C.B., de Castro Miguel, E., de Carvalho Leitão, R.F., da Silva Costa, D.V. and Cruz, L.J. Spherical neutral gold nanoparticles improve anti-inflammatory response, oxidative stress and fibrosis in alcohol-methamphetamine-induced liver injury in rats. International journal of pharmaceutics. 2018; 548(1): p. 114-.

42. Ibrahim, K.E., Al-Mutary, M.G., Bakhiet, A.O. and Khan, H.A. Histopathology of the Liver, Kidney and Spleen of Mice Exposed to Gold Nanoparticles. Molecules. 2018; 23(8): p. 1848.

43. Doudi, M. and Setorki, M. The acute liver injury in rat caused by gold nanoparticles. Nanomedicine Journal. 2014; 1(4): p. 248257-.

44. Zhang, Y., Wang, P., Wang, Y., Li, J., Qiao, D., Chen, R., Yang, W. and Yan, F. Gold Nanoparticles Promote the Bone Regeneration of Periodontal Ligament Stem Cell Sheets Through Activation of Autophagy. International journal of nanomedicine. 2021; 16: p. 6173-.

45. Ebaid, H., Dkhil, M.A., Danfour, M.A., Tohamy, A. and Gabry, M.S. Piroxicam-induced hepatic and renal histopathological changes in mice. Libyan Journal of Medicine. 2007; 2(2): p. 8289-.

46. Ahmad, A., Nawaz, R.S., Qureshi, T.A., Nizamani, Z.A., Rao, N., Qasim, M. and Ali, A. Histopathological effect of Meloxicam (Preferential COX-2 inhibitor NSAID) on liver and kidney of Rabbit. International Journal of Biosciences. 2017; 11(3): p. p. 148158-.

47. Machlus, K.R. and Italiano, J.E., Jr. The incredible journey: From megakaryocyte development to platelet formation. Journal of Cell Biology. 2013; 201(6): p. 785796-.

الملخص العربي

تخفف جزيئات الذهب المتناهية الصغر التسمم المحدث بالميلوكسيكام في طحال ذكر الجرذ البالغ عن طريق تنشيط الإلتهام الذاتي: دراسة نسيجية وكيمياء نسيج مناعية

شيرين أحمد محمد[١]، حكمت عصمان عبد العزيز[١]، عزيز عواد[٢]، سميرة محمود محمد[١]

١قسم الهستولوجي، كلية الطب، جامعة سوهاج

٢قسم علم الحيوان، كلية العلوم، جامعة سوهاج

مقدمة: الميلوكسيكام يعمل كمسكن ذو درجة تثبيط عالية لانزيم COX2. مما يؤدي إلى الإجهاد التأكسدي. جسيمات الذهب المتناهية الصغر لها العديد من التطبيقات الطبية في تشخيص الأمراض وعلاجها ولها خصائص قوية لإزالة الشوارد الحرة.

الهدف من الدراسة: أجريت هذه الدراسة لتقييم التأثير العلاجي المحتمل لـجسيمات الذهب المتناهية الصغر على سمية الطحال التي يسببها الميلوكسيكام في نقاط زمنية مختلفة.

أدوات وطرق البحث: تم استخدام خمسة وأربعين جرذاً في هذه التجربة وتم تقسيمها إلى ثماني مجموعات: المجموعة الأولى: المجموعة الضابطة، والمجموعة الثانية: تم حقن الحيوانات بـجسيمات الذهب المتناهية الصغر لمدة أسبوعين. تلقت المجموعات المعالجة بالميلوكسيكام بجرعة (١٥ مجم / كجم) يوميًا عن طريق الحقن داخل الصفاق لمدة أسبوعين في المجموعة الثالثة وشهرين في المجموعة الرابعة. تم حقن المجموعات المعالجة بجسيمات الذهب المتناهية الصغر لمدة أسبوعين بعد تلقي الميلوكسيكام لمدة أسبوعين في المجموعة الخامسة وشهرين في المجموعة السادسة، توقف العلاج بالميلوكسيكام لمدة أسبوعين بعد تجرعه لمدة أسبوعين في المجموعة السابعة وشهرين في المجموعة الثامنة. تمت دراسة التغيرات النسيجية وتحديد مكان تمركز جسيمات الذهب المتناهية الصغر داخل الطحال بواسطة نترات الفضة، وتحديد التعبير النسيجى الكيمياء- مناعي لـمضادات ال PCNA للكشف عن التكاثر الخلوي، وLC3 وp62 للكشف عن نشاط الإلتهام الذاتي.

النتائج: لوحظ أن التغيرات النسيجية التنكسية وزيادة تعبير PCNA وLC3 وp62 أكثر وضوحًا في مدة شهرين من العلاج بالميلوكسيكام . ومع ذلك، حسنت جسيمات الذهب المتناهية الصغر هذه التغييرات.

الخلاصة: نجسيمات الذهب المتناهية الصغر لها تأثير علاجي ضد التأثيرات السامة لـعقار الميلوكسيكام في الطحال والذي قد يكون بسبب دورها كمضاد للأكسدة، بالإضافة إلى تنشيط الالتهام الذاتي.